AIG Journal
Published by the Australian Institute of Geoscientists
ISSN 1443-1017

The Inca uraniferous skarn, Namibia: an unusual magmatic-hydrothermal deposit

Andy Wilde

Centre for Exploration Targeting, University of Western Australia, Crawley, WA, Australia.
drandyrwilde@gmail.com

Abstract

Inca is a skarn-hosted magmatic-hydrothermal uranium deposit located in the Erongo district of Namibia. It differs in several key ways from typical intrusive uranium deposits of the region, principally because uranium occurs in skarn rather than in leucogranite intrusions. Preliminary observations presented here suggest that Inca is the product of the separation of a uraniferous hydrothermal fluid from leucogranite magma. This was the result of magma interacting with marble as hypothesized by Cuney (1980). Inca is one of only two economically significant skarn-hosted uranium deposits in the world. The other is the Mary Kathleen deposit, near Mount Isa in Queensland. Uranium deposition at Inca is paragenetically linked to skarn formation. At Mary Kathleen, however, uranium was introduced over 200 Ma after the formation of the host skarns. Inca is thus unique.

Introduction

The Erongo uranium region, east of Swakopmund in Namibia, is one of the world's leading uranium producing regions with three major mines either in production or under construction. The region is well known for its substantial endowment of leucogranite-hosted "intrusive" uranium deposits[1] exemplified by Rössing and Husab (Figure 1, Table 1; Berning et al., 1968). Inca, however, is a very different style of deposit and appears to be one of only two significant skarn-hosted uranium deposits in the world, the other being Mary Kathleen in Queensland. Inca was discovered in 2009 by drilling along strike of a weak airborne radiometric uranium anomaly coincident with a small pit ("Von Stryk" pit) that yielded a few tonnes of impure magnetite. Inca has a combined inferred and indicated resource of 12.4 Mt at 490 ppm U3O8 at a 250 ppm cutoff (http://www.deepyellow.com.au/namibia-development/inca-deposit.html). The deposit remains open in several directions.

This contribution provides a preliminary description of the Inca deposit and highlights some features that are suggestive of the involvement of hydrothermal fluids in its formation. This mode of formation is in contrast to the intrusive deposits of the region that are considered to be of purely magmatic origin (Cuney, 1980; Nex, 1997; Nex et al., 2002; Kinnaird & Nex, 2007). Observations presented here are based primarily from outcrop in the vicinity of the deposits, and on logging of numerous diamond and reverse circulation drill holes. These data are supplemented by optical microscopy (Purvis, 2008) and quantitative evaluation of minerals by scanning electron microscopy (QEMSCAN, Hodgson, 2009).

Regional Geological Setting

The Erongo region consists of four main geological units. These are Palaeoproterozoic to Mesoproterozoic gneisses, Neoproterozoic gneisses, marbles and skarn, Neoproterozoic to Cambrian (Pan-African) felsic intrusions, and unconformable Cenozoic sediments. Paleoproterozoic to Mesoproterozoic gneisses (Abbabis metamorphic complex) occur as several inliers or domes overlain by Neoproterozoic rocks with the contact typically marked by a high strain zone (Cuney, 1980; Basson & Greenway, 2004; Kinnaird & Nex, 2007).

[1] *"Intrusive" is an International Atomic Energy Agency classification. The deposit type is also known as alaskite-type or alaskite-hosted.*

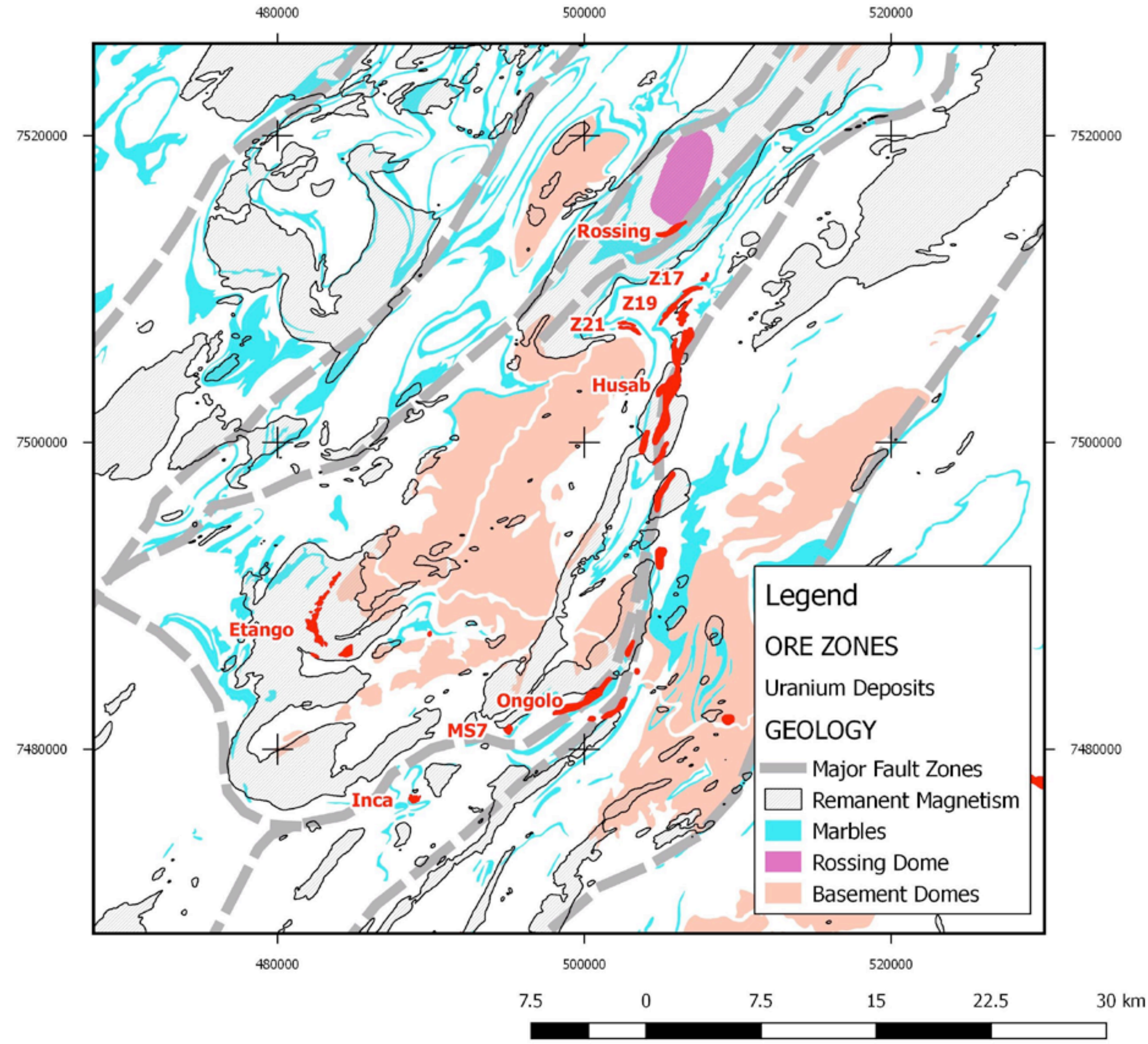

Figure 1. Key geological features of the Erongo uranium district. Geology from the Geological Survey of Namibia. The association between uraniferous leucogranite and remanent magnetization was first documented by Corner (1983). Faults based on unpublished interpretations of Klaus Knupp.

Many intrusive uranium deposits are spatially associated with this contact and are hosted by Neoproterozoic rocks of the Khan and Rössing Formations (Basson & Greenway, 2004). The Khan Formation consists of amphibole-, diopside- and carbonate-rich gneisses, locally with high volumes (up to 20%) of pre-metamorphic anhydrite (Nash, 1972; Cuney, 1980; Sawyer, 1981). The Rössing Formation consists of marble, meta-conglomerate, quartzite, cordierite gneiss and a variety of skarn rocks (Kinnaird & Nex, 2007).

The Proterozoic rocks underwent a major compressive deformation event (D_2) at 550 ± 10 (Longridge, 2012). This D_2 event established a pervasive NE-SW fabric and recumbent to shallow NW-dipping folds accompanied by granulite facies metamorphism and partial melting (Longridge, 2012).

Table 1. Uranium resources of intrusive uranium deposits of the Erongo region of Namibia. Sourced from respective company websites and NI43-101 reports. Note the Inca resource is quoted at a 100 ppm cut-off.

Deposit	Million Tonnes Ore	Grade Ore (% U_3O_8)	Contained U_3O_8 (tonnes)	Contained U_3O_8 (Mlbs)
HUSAB	331	0.04	132,450	292
RÖSSING	-	-	>55,790	>123
ETANGO	500	0.02	96,200	212
ROSSING Z20	202	0.03	54,540	120
VALENCIA	161	0.02	30,850	68
INCA	37	0.03	10,000	22
ONGOLO	21	0.04	8,230	18
GARNET VALLEY	26	0.03	6,817	15
MS7	7	0.04	2,970	7

Late in D_2, the dominantly compressive deformation switched to NE-SW directed extension which formed shear zones on fold limbs and at the boundaries of Abbabis complex domes (Figure 1; Basson & Greenway, 2004; Longridge, 2012). This change from compression to extension probably triggered intrusion of the extensive "Salem" suite of foliated granodiorites, granites and adamellites at 555 ± 5 Ma, and potassium-rich granites ("Red Granites") at 535 ± 8 Ma (Briqueu et al., 1980 Sawyer, 1981; Marlow, 1981; Kroner, 1982; Miller, 1983; Nex, 1997; Longridge, 2012).

Intrusive-type uranium deposits are related to a third suite of dominantly leucogranitic rocks at approximately 510 Ma (Briqueu et al., 1980; Nex, 1997; Nex et al., 2002). Intrusion of this Cambrian leucogranite suite occurred during D_3 deformation which is the product of north–south directed transpression (Basson & Greenway, 2004; Longridge, 2012). Leucogranite intrusions vary in form from transgressive sheeted dykes (Figure 2a) to intrusive breccias (Figure 2b). The distribution of the intrusions is not well mapped, due partly to the complexity of individual intrusions. Areas of remanent magnetism, however, define the location of substantial bodies of leucogranite (Fig. 1; Corner, 1983). Most of the significant deposits occur within areas of remanent magnetism (Corner, 1983).

The next major geological event recorded in the region is the development of a network of Cenozoic palaeodrainages incised into the Proterozoic basement. These palaeodrainages were filled by coarse clastic sediments which now host secondary (surficial) uranium deposits such as that at the Langer Heinrich mine.

Geology of the Inca Deposit

Host Lithologies

Outcrop at Inca is poor, with the exception of a layer of calcite marble which forms the footwall to uranium mineralisation. Drilling shows that the deposit is hosted within a variety of rocks situated in the hanging wall of the marble (Figure 3). These rocks range from biotite and amphibole-rich gneiss to a variety of skarns intruded by texturally variable leucogranite intrusions. Approximately 50% of the rock volume at Inca comprises such intrusions. Leucogranite intrudes both metamorphic rocks and skarn.

Typical intersections at Inca are shown in the form of strip logs as Figure 4. Biotite- and amphibole-rich gneisses are the dominant protoliths, with biotite-rich gneiss being most abundant near to the marble contact. Both units contain numerous thin layers of black garnetite (near monomineralic garnet rocks, Figure 5a,b) and a range of amphibole- or clinopyroxene-rich and iron oxide-rich skarns.

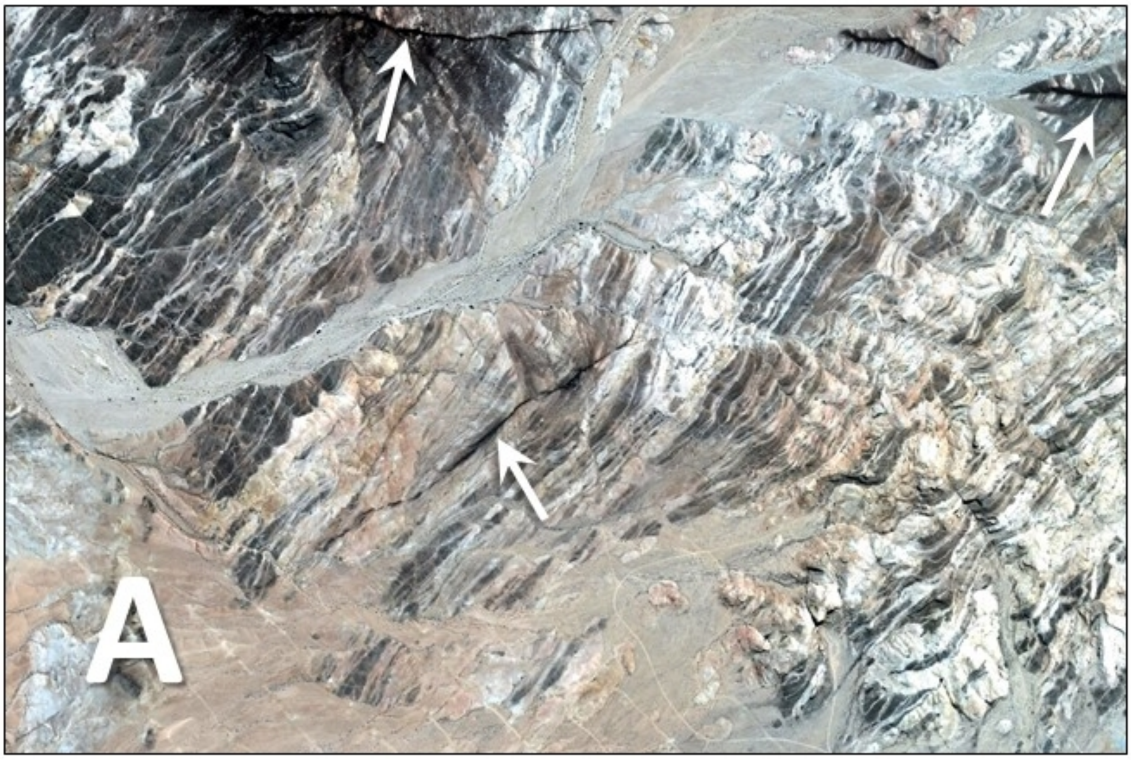

Figure 2. Spot image of the area north of the Ongolo deposit illustrating the geometry of leucogranite intrusions, namely numerous parallel sheets of different thickness. Arrows show Karoo-aged (i.e. post ore) dykes. B – Outcrop of leucogranite intrusion in the Holland Dome area. In this case, the intrusion defines a mega-breccia.

The iron oxide-rich rocks vary from massive, to incipient breccia (Figure 5c) to breccias in which isolated and rounded iron oxide fragments are supported by coarse, vuggy calcite and nontronite (iron-rich smectite) and goethite (Figure 5d). The iron oxide-rich skarns contain varying proportions of magnetite, hematite and ilmenite and textural evidence suggests that hematite replaces magnetite (Purvis, 2008). Hematite also occurs as exsolution lamellae in ilmenite (Purvis, 2008).

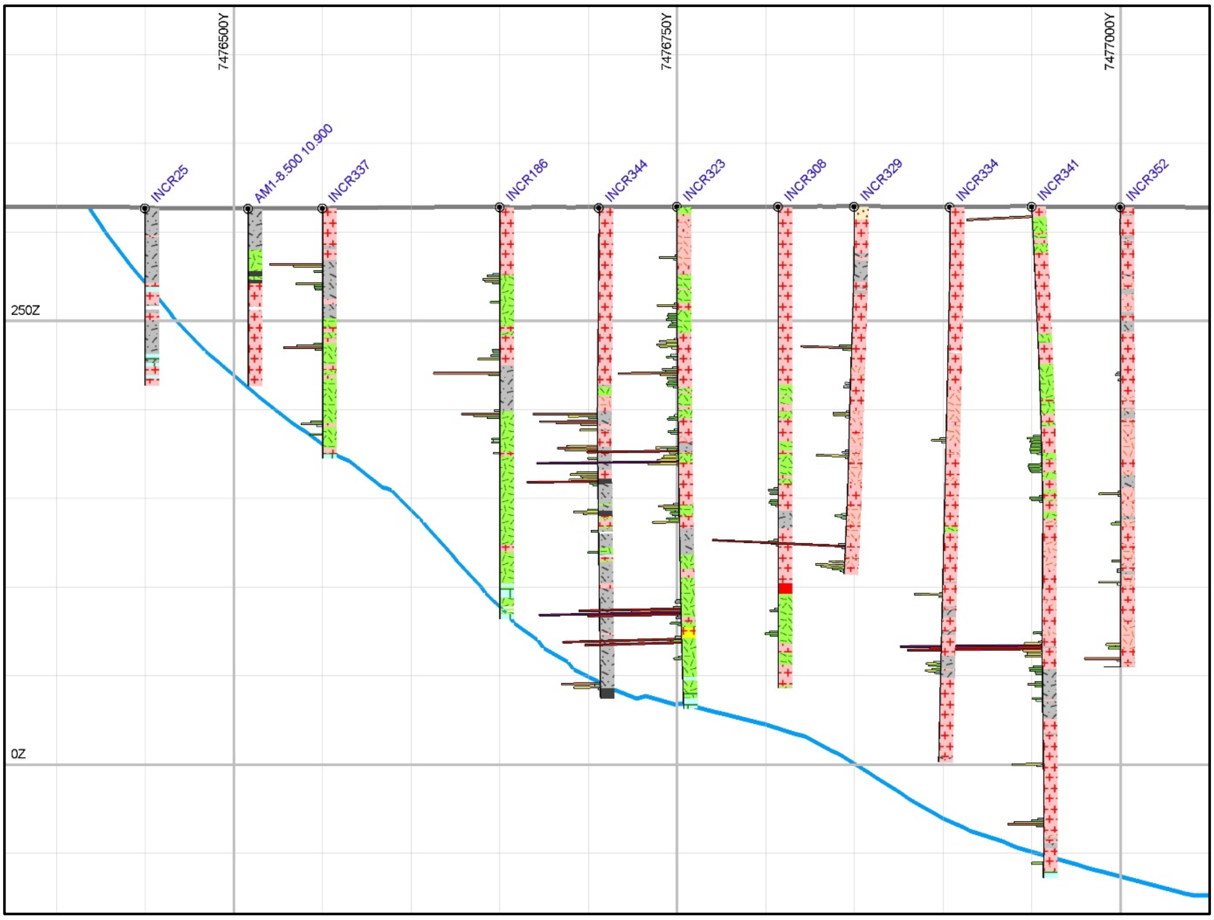

Figure 3: Typical cross section of the Inca deposit. Y and Z co-ordinates in metres. Histograms show uranium grade by assay. Blue line is upper marble contact. "Granite" in pink, "calc-silicate gneiss" in green and "quartz-biotite gneiss" in grey. Skarn lithologies were not differentiated during logging by company geologists. The logging codes differ from those used by the author in Figure 4. Difficulty in correlating units between adjacent drill holes is universal in the hard-rock uranium deposits of the Erongo region and stems partly from complex intrusive geometry such as that illustrated in Figure 2b.

Intervals logged as "altered rocks" in Figure 4 contain a high volume of disseminated carbonate. Calcite veining is particularly prevalent in the iron oxide-rich rocks (Fig. 5c). Calcite veins and encloses Fe- and Ti-oxide and therefore is paragenetically later. Calcite has an unusual platy texture reminiscent of textures observed in epithermal gold deposits and probably indicative of rapid cooling, perhaps the result of boiling of an aqueous fluid (Figure 6; Purvis, 2008). Interstices between platy calcite crystals are infilled by goethite and by radiating yellow-green crystals tentatively identified as nontronite. Both phases may be significantly younger than the calcite.

Figure 4 illustrates another significant feature of the mineralization at Inca, namely that very little economic uranium is hosted within leucogranite intrusions. This sets Inca apart from intrusive deposits such as Rössing and Husab where the reverse is true. An anomalous uranium content of between 50 and 100 ppm is, however, not uncommon in the Inca leucogranites (Figure 4). Higher uranium grades occur in a wide variety of host-rocks but over thicknesses of only a few meters. Iron-oxide rich rocks contain some of the highest uranium grades at Inca, typically between 500 and 1,000 ppm U_3O_8 and rarely up to 1%. In many cases, the presence of thin high grade zones can be related to the contact between lithologically and presumably mechanically distinct units (Figure 4).

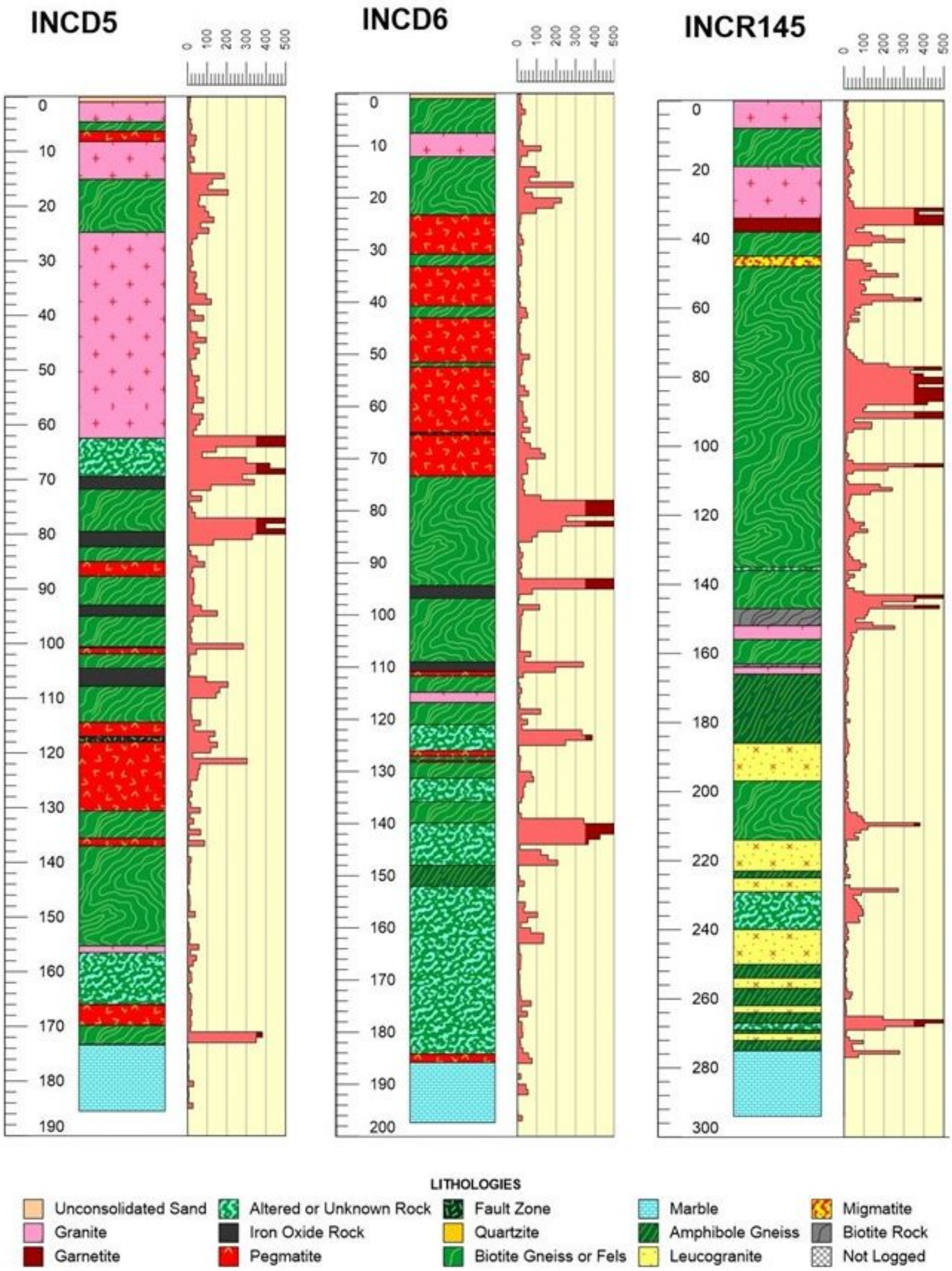

Figure 4. Representative strip logs of diamond drill holes from Inca. The histograms are uranium content as ppm U_3O_8. Garnetite, iron oxide rock and "altered or unknown rock" are varieties of skarn. Many other types of skarn rocks were not differentiated from the host, partly because amphibole- or pyroxene-rich skarn is patchily developed.

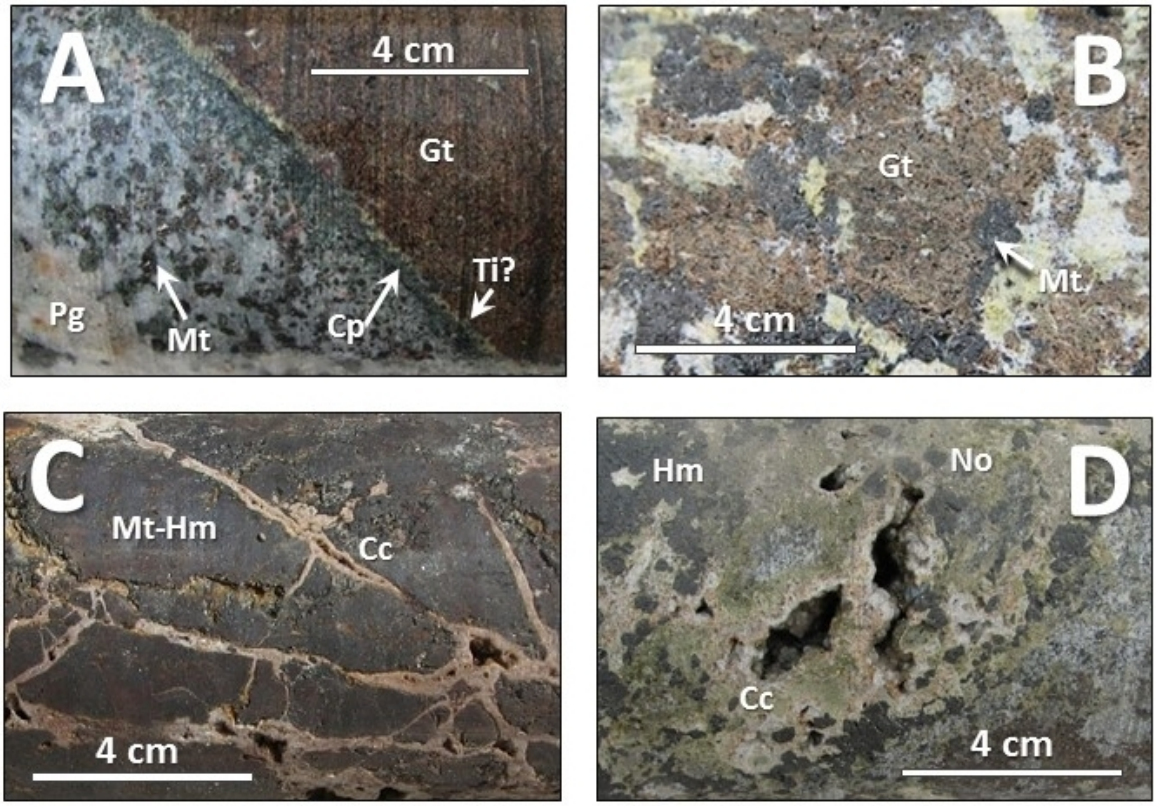

Figure 5. Images of outcrop and core from Inca. A - Contact between pegmatite (Pg, left) and garnetite (Gt, right). Magnetite (mt) is enriched at the contact zone and there is a thin rind of clinopyroxene (cp) and a possible Ti oxide (Ti?) right at the contact; B - Residual garnetite (gt) with magnetite (mt) rims; C - Massive magnetite-hematite rock cut by vuggy calcite-nontronite veins. D - Close-up of vuggy calcite-nontronite breccia cement.

Mineralization Styles

Three distinct textural and mineralogical types of uranium mineralization are currently recognised, but the spatial distribution of these ore types at the orebody scale is poorly defined. Type I mineralization consists of uranium disseminated in various skarn rocks. Optical microscopy and QEMSCAN reveal rounded, 100 to 200 micron-scale grains of uraninite within feldspar, clinopyroxene, amphibole, and magnetite (Figure 7a; Purvis, 2008; Hodgson, 2009). This mode of occurrence is reminiscent of that in intrusive-type deposits, where much uranium occurs as morphologically identical inclusions in silicates, particularly feldspar (Berning et al., 1968). It can be inferred that Type I uranium formation at Inca occurred relatively early in the metasomatic history and is paragenetically associated with formation of primary skarn minerals.

Type II ore is defined by a high density of calcite veinlets. Uraninite and coffinite have been identified with some certainty and have an average grain size of 20 and 4 microns respectively (Figure 7b-d). QEMSCAN also reported many instances of “uranium silicate” or “uranium silicate intergrowths” with grain size of less than 2 microns: brannerite or other U-Ti phases are rare. Type II uranium phases occur as microveinlets in magnetite, hematite, and calcite (Figure 7b-d). This textural relationship places Type II uranium precipitation at a late stage relative to both Type I uranium and the crystallization of magnetite and calcite. The relative abundance of Types I and II mineralization is not currently known.

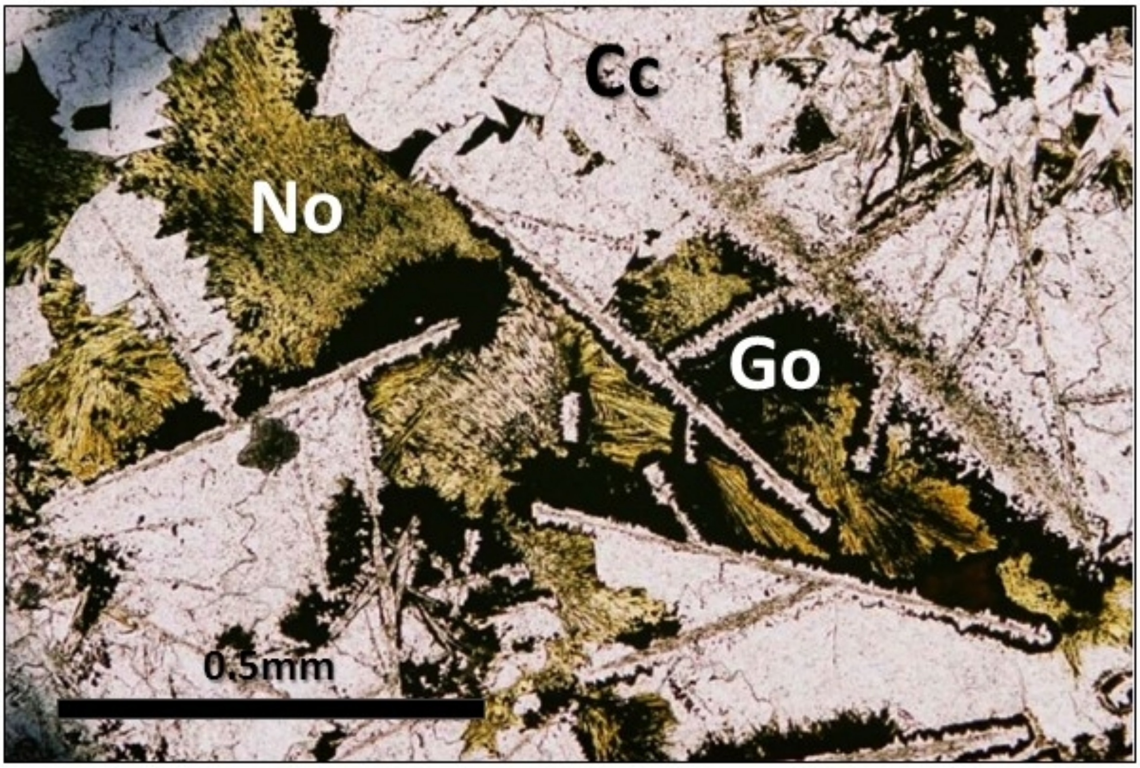

Figure 6. Photomicrograph (transmitted light) of unusual bladed calcite in breccia matrix. Infill of greenish nontronite and black iron oxide or hydroxide.

Rare Type III ore consists of secondary uranium minerals (including autunite) in clay and iron hydroxide-lined fractures mainly in granitoids in the upper parts of the Inca orebody. This ore type is probably supergene in origin. Type III ore appears to be relatively rare at Inca, but at Rossing a similar secondary enrichment accounts for a significant portion of the high-grade ore (Berning et al., 1968).

Discussion

Intrusive-Type Uranium Deposits

Intrusive uranium deposits of the Erongo region are commonly believed to be the product of post-tectonic leucogranite magmatism at about 510 Ma (Von Backstrom, 1970; Cuney, 1980; Briqueu et al., 1980; Nex, 1997; Kinnaird & Nex, 2007; Corvino and Pretorius, 2008). In these deposits, uranium is generally restricted to pegmatitic leucogranite veins or dykes that intrude high grade metamorphic host rocks, and to the adjacent biotite-rich selvages. Minor skarn intersections are not uncommon at these deposits, but these seldom carry significant uranium grades.

Proximity to marble layers has been suggested to be a crucial feature of ore genesis (Cuney, 1980; Corvino and Pretorius, 2008). This could be due to "ponding" of upwards magma flow by impenetrable marble layers (Corvino and Pretorius, 2008) or to chemical assimilation of marble and consequent increase in the activity of CO_2 in the magma (Cuney, 1980). The former is improbable because marble layers were probably steeply dipping at the time of intrusion. Cuney (1980) argued that build-up of CO_2 would have resulted in phase separation encouraging immediate and in-situ crystallization of the magma. If the magma remained reduced (close to Ni-NiO buffer) uranium would have remained in the magma rather than a CO_2-rich vapour phase (Cuney, 1980).

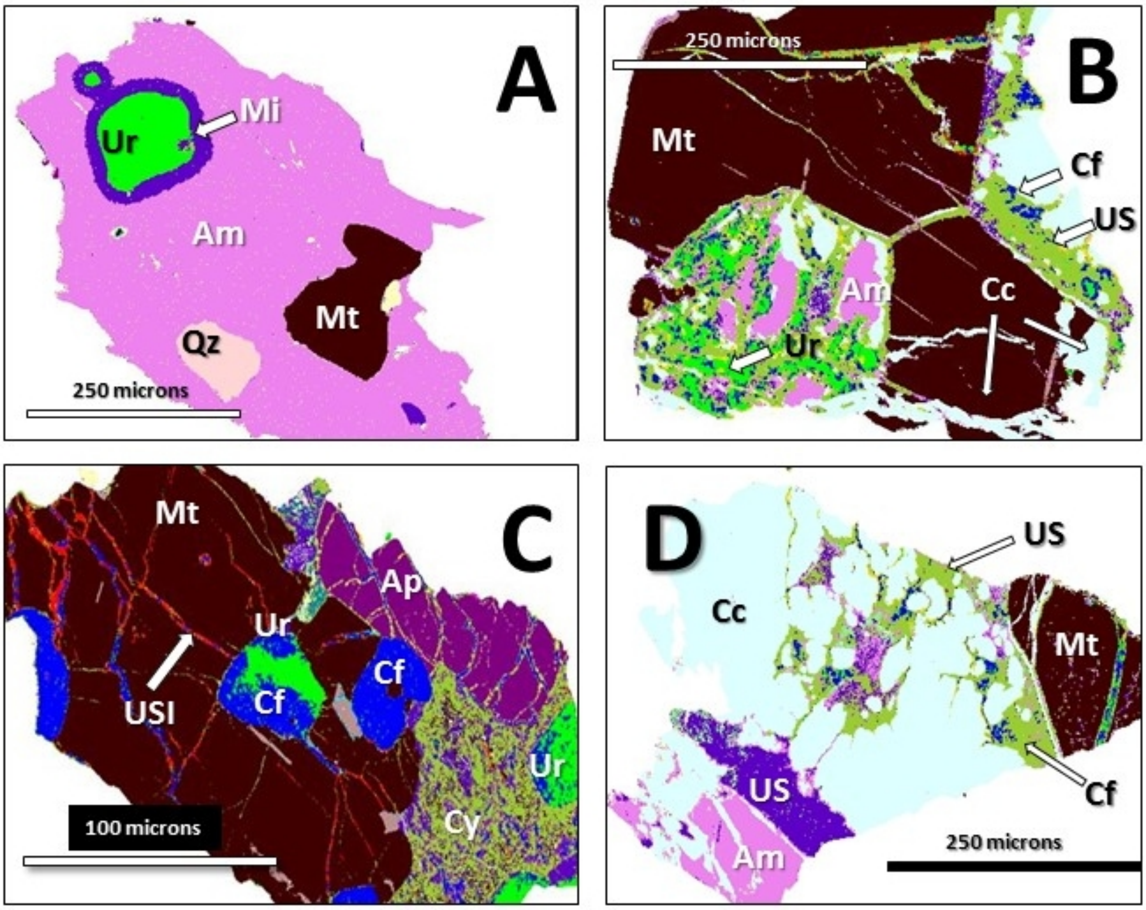

Figure 7. QEMSCAN images of Inca ore. A - Early uraninite (Ur) in amphibole with biotite (Mi) rim. The amphibole also has inclusions of quartz (Qz) and iron oxide (Mt). B - Uraninite in iron oxide (Mt) showing later veining and possible remobilization as uranium silicates (US). CC – calcite. Cf – coffinite. C - Uraninite-coffinite in magnetite with late unidentified uranium silicate intergrowth (USI) veinlet. Ap – apatite. D - Unidentified uranium silicate (US) veining and replacing calcite (Cc), amphibole (Am) and magnetite (Mt).

Under more oxidizing conditions, for example if the magma equilibrated with anhydrite-rich gneiss, uranium would have partitioned into the CO_2-H_2O phase (Cuney, 1980). Until the discovery of Inca, no evidence had been found which might indicate the presence of a CO_2-rich hydrothermal vapour phase or its derivatives. Inca appears to provide substantial support for Cuney's (1980) hypothesis.

A Magmatic-Hydrothermal Model for Inca

Clearly the purely intrusive model does not apply at Inca, although Inca shares with many intrusive uranium deposits a strong spatial association with a marble contact. Much of the uranium at Inca is hosted by lithologies other than magmatic ones and in many (though not all) cases is associated with high densities of calcite vein and breccia matrix.

There is textural evidence of two uranium depositing events. The earliest event (Type I) was contemporaneous with skarnification of Proterozoic carbonate-rich gneisses, since uranium occurs as inclusions in primary skarn minerals The second event (Type II) is defined by paragenetically late uranium silicates associated with calcite veining, often spatially associated with iron oxide rich host-rocks. There is clear evidence of Type II uranium phases replacing Type I inclusions. Bladed calcite crystals indicate that calcite formation is due to rapid, possibly catastrophic, cooling as might be the result of CO_2 exsolution from the magma as envisaged by Cuney (1980).

A strong association between the larger alaskite-type deposits such as Rossing and Husab with major regional fault (shear) zones is shown in figure 1. Inca differs in being apparently unrelated to a major shear and remote from domal contacts. Inca may therefore be a more distal style of deposit that formed in a different (local) stress regime than the alaskite-type deposits. Targeting similar deposits could involve looking at areas on the flanks of remanently magnetized zones, and distal to domal boundaries and major structures.

Comparison to Mary Kathleen

The Mary Kathleen deposit is the only other economically significant skarn-hosted uranium deposit in the world. The Mary Kathleen mine operated between 1958 and 1982 and produced approximately 8,900 tonnes of U_3O_8 from skarn-hosted ore (Wilde et al., 2013). The ore was enriched in rare earth elements; however, these were not recovered. Skarn rocks are rich in pyroxene and garnet, and were formed in response to the intrusion of the 1750 to 1730 Ma Burstall Granite (Page 1983; Pearson et al. 1992; Maas et al. 1988; Oliver et al., 1999).
Uranium, however, is paragenetically associated with a much later event that overprinted primary skarn (Oliver et al., 1999). High-grade mineralisation occurs as uraninite-bearing allanite and secondary garnet veins (Oliver et al., 1999). Altered massive garnet skarn has been dated at 1580 ± 50 Ma (Maas et al. (1988). It is quite clear, therefore, that uranium at Mary Kathleen was introduced much later than intrusion of the Burstall Granite and attendant skarnification of its host-rocks. This is the reverse of the case at Inca, where at least a portion of the uranium is contemporaneous with formation of skarn minerals.

Uranium and REE ore formation at Mary Kathleen has been attributed to transport in and deposition from a large-scale metamorphic fluid system although with a possible (yet to be confirmed) contribution from younger granitoids (Oliver et al., 1999). A key aspect of ore genesis is that the primary skarn body acted as a major zone of mechanical inhomogeneity that allowed focusing of uraniferous fluids, be they of metamorphic or magmatic origin (Oliver et al., 1999).

Conclusions

Inca is a unique skarn-hosted magmatic-hydrothermal uranium deposit. It differs in several key ways from typical intrusive uranium deposits of the Erongo region of Namibia, notably in the absence of significant uranium grades in leucogranite intrusions. Evidence advanced here suggests that Inca is the product of the evolution of a magmatic hydrothermal fluid as leucogranite magma interacted with marble as hypothesized by Cuney (1980). Inca is quite different to the Mary Kathleen skarn-hosted deposit as uranium deposition is paragenetically linked to skarn formation, whereas as Mary Kathleen uranium was introduced over 200 Ma after the formation of skarns. At Mary Kathleen the significance of the skarn rocks was in the creation of an inhomogeneous rock mass that allowed the focusing of extraneous hydrothermal fluids (Oliver et al., 1999).

References

Basson I.J. and Greenway G., 2004, The Rossing Uranium Deposit: a product of late-kinematic localization of uraniferous granites in the Central Zone of the Damara Orogen, Namibia: Journal of African Earth Sciences, V.38, pp. 413–435.

Berning J., Cooke R., Hiemstra S.A. and Hoffman U., The Rossing uranium deposit, south-west Africa: Econ. Geol., V71, 1976, pp. 351-368.

Briqueu L., Lancelot J., Valois J-P. and Walgenwitz F., 1980, Geochronologie U-Pb et genese d'un type de mineralisation uranifere: les alaskites de Goanikontes (Namibie) et leur encaissant: Bull. Centre Rech. Explor. Prod. Elf. Aquitaine, V.4, pp. 759–811.

Corner B., 1983, An Interpretation of the Aeromagnetic Data Covering the Western Portion of the Damara Orogen in South West Africa/Namibia: Spec. Pub. Geol. Soc. Africa., V.11, pp. 339-354.

Corvino A. and Pretorius L., 2013, Uraniferous leucogranites south of Ida Dome, central Damara Belt, Namibia: morphology, distribution and mineralisation: Journal of African Earth Sciences, V.80, pp. 60–73.

Cuney M., 1980, Preliminary Results on the Petrology and Fluid Inclusions of the Rossing Uraniferous Alaskites: Trans. Geol. Soc. South Africa., V83, pp. 39-45.

Hodgson W., Report for Deep Yellow on QEMSCAN Analysis: SGS Lakefield Oretest, 2009.

Kinnaird J.A. and Nex P., 2007, A review of geological controls on uranium mineralisation in sheeted leucogranites within the Damara Orogen, Namibia: Trans. IMM B, V.116, pp 68-76.

Kröner, A., 1982, Rb-Sr geochronology and tectonic evolution of the Pan-African Damara belt of Namibia, south-western Africa: American Journal of Science, V.282, pp. 1471-1507.

Longridge L., 2012, Tectonothermal Evolution of the southwestern Central Zone, Damara Belt, Namibia: PhD Dissertation, Faculty of Science, University of the Witwatersrand, Johannesburg, 563pp.

Maas R., McCulloch M. T. and Campbell I. H. 1988. Sm–Nd isotope systematics in uranium rare-earth element mineralization at Mary Kathleen uranium mine, Queensland. Economic Geology V.82, pp. 1805–1826.

Marlow, A., 1981, Remobilisation and Primary Uranium Genesis in the Damaran Orogenic Belt: PhD Thesis, University of Leeds, 247 pp.

Miller R.M., 1983, Evolution of the Damara Orogen of southwest Africa/Namibia, Special Publication Geological Society of South Africa, Johannesburg, 11, 515 pp.

Nash C.R., 1972, Primary Anhydrite in Precambrian Gneisses from the Swakopmund District, South West Africa: Cont. Min. Pet., V.36, pp. 27-32.

Nex P., Herd D. and Kinnaird J., 2002, Fluid extraction from quartz in sheeted leucogranites as a monitor to styles of uranium mineralization: an example from the Rössing area, Namibia: Geochemistry: Exploration, Environment, Analysis, V.2, pp. 83–96.

Nex, P., 1997, Tectono-metamorphic setting and evolution of granitic sheets in the Goanikontes area, Namibia: PhD Thesis, Department of Geology, National University of Ireland, Cork, 322 pp.

Oliver N.H.S., Pearson P. J., Holcombe R. J and Ord A., 1999, Mary Kathleen metamorphic–hydrothermal uranium – rare-earth element deposit: ore genesis and numerical model of coupled deformation and fluid flow: Australian Journal of Earth Sciences, V.46, pp. 467–484.

Page R. W. 1983. Chronology of magmatism, skarn formation and uranium mineralisation, Mary Kathleen, Queensland, Australia. Economic Geology V.78, pp. 838–853.

Pearson P. J., Holcombe R. J. & Page R. W., 1992. Synkinematic emplacement of the Middle Proterozoic Wonga Batholith into a mid-crustal extensional shear zone, Mount Isa Inlier, Queensland, Australia. In: Stewart A. J. & Blake D. H. eds. Detailed Studies of the Mount Isa Inlier, Australian Geological Survey Organisation Bulletin 243, pp. 289–328.

Purvis A., 2008, Mineralogical Report No.9326, Unpublished Report for Deep Yellow Ltd., Pontifex & Associates, 37pp.

Sawyer E., 1981, Damaran structural and metamorphic geology of an area south-east of Walvis Bay, South West Africa/Namibia. Memoir of the Geological Survey of South West Africa, V.7, 94 pp.

Von Backstrom J.W., 1970, The Rossing uranium deposit near Swakopmund, South-West Africa. A preliminary report: Uranium Exploration Geology, IAEA, Vienna, pp. 143-150.

Wilde A.R., Otto A., Jory J., MacRae C., Pownceby M., Wilson N. and Torpy A., 2013 Geology and Mineralogy of Uranium Deposits from Mount Isa, Australia: Implications for Albitite Uranium Deposit Models: Minerals, V.3, pp. 258-283.

AIG Journal Paper N2016-002
Received 4 October 2016
Reviewed: 28 October 2016
Accepted: 28 October 2016
Published: 20 March 2017